Energy Fuels **2010,** *24,* 1207–1212 · DOI:10.1021/ef900694z
Published on Web 01/29/2010

energy&fuels
article

Continuous Formation Process of CO_2 Gas Hydrate via a Vortex and Impinging Stream Reactor

Jing Bai,[†,‡] Deqing Liang,*[,†] Dongliang Li,[†,‡] Shuanshi Fan,[§] Jianwei Du,[†,‡] Xingxue Dai,[†,‡] and Zhen Long[†,‡]

[†]*Key Laboratory of Renewable Energy and Natural Gas Hydrate, Guangzhou Institute of Energy Conversion, Chinese Academy of Science, Guangzhou 510640, China,* [‡]*Graduate School of Chinese Academy of Science, Beijing 100039, China, and* [§]*South China University of Technology, Guangzhou 510640, China*

Received July 4, 2009. Revised Manuscript Received January 4, 2010

A continuous formation process of CO_2 hydrate was investigated in a vortex and impinging stream reactor (VIR) of 1.76 L with the temperatures ranging from 274.46 to 275.86 K and the pressures ranging from 1.79 to 3.163 MPa. In the VIR, a high-gravity field can be generated, where both centrifugal and impinging forces can intensify the mass transfer in reactants. There are two distinct steps in the process. The first step is the unstable hydrate formation process. The next one is called the stable formation process, which presents the rapid and continuous formation of the CO_2 gas hydrate. It is found that the formation rate of CO_2 hydrate is up to 249.8 mol/h when the Higee factor β is 390.28.

1. Introduction

Gas hydrates are ice-like solids that are formed when guest molecules are trapped inside cage-like structures of water molecules. Gas hydrates draw much attention, not only because there are significant energy resources in the form of hydrates below the ocean floor or in the permafrost regions but also because a series of new technologies can be developed on the basis of them, including separation of the gas mixture by forming and dissociating hydrate, the storage of natural gas in the form of hydrate, desalination of seawater through hydrate formation, etc.[1,2] Especially, CO_2 hydrates are of particular interest as a medium for marine sequestration of anthropogenic CO_2 currently, and properties of CO_2 hydrates have been studied as a mitigation measure for global warming.[3,4] However, the effect of CO_2 hydrates should be considered with regard to the design of the injection of liquid CO_2 and the prediction of the fate of CO_2 sequestered in the seawater, because the hydrate is thermodynamically stable in ocean depths of more than 450 m.[5] Besides, natural gas hydrate (NGH) was originally proposed as a viable alternative to liquefied natural gas (LNG), compressed natural gas (CNG), or pipelined natural gas (PNG) for transportation of natural gas from the source to the demand by Gudmundsson and Børrehaug.[6] Therefore, it has stimulated intensive research in this field. On the other hand, an economic evaluation of NGH as an alternative for natural gas transportation has been given by Javanmardi and Najibi.[7,8] Their results show that NGH has many advantages over LNG, CNG, and PNG in some cases.

How to form hydrates rapidly and continuously is a concern in the development and industrialization of the above technologies based on hydrates. Many methods have been proposed to promote the hydrate formation. For example, a certain quantity of additives or materials have been used as accelerants, such as sodium dodecyl sulfate (SDS), alkylpolyglucoside (APG), Tween, dry water, etc.[9−14] Besides, researchers have reported some mechanical methods, such as stirring, spraying of liquid, bubbling of gas, etc. These methods correspond to the different types of reactors, stirred tanks,

*To whom correspondence should be addressed. Telephone: +(86)20-87057669. Fax: +(86)20-87057669. E-mail: liangdq@ms.giec.ac.cn.

(1) Sloan, E. D. *Clathrate Hydrates of Natural Gases*; Marcel Dekker: New York, 1998.
(2) Englezos, P. Clathrate hydrates. *Ind. Eng. Chem. Res.* **1993**, *32*, 1251–1274.
(3) Løken, K. P.; Austvik, T. Deposition of CO_2 on the seabed in the form of hydrates, part II. *Energy Convers. Manage.* **1993**, *34*, 1081–1087.
(4) Lund, P. C. The effect of CO_2−hydrates on deep ocean carbon dioxide deposition options. *Energy Convers. Manage.* **1995**, *36*, 543–546.
(5) Yamasaki, A.; Wakatsuki, M.; Teng, H.; Yanagisawa, Y.; Yamada, K. A new ocean disposal scenario for anthropogenic CO_2: CO_2 hydrate formation in a submerged crystallizer and its disposal. *Energy* **2000**, *25*, 85–96.
(6) Gudmundsson, J. S.; Børrehaug, A. Frozen hydrate for transport of natural gas. Proceedings of the 2nd International Conference on Natural Gas Hydrates, Toulouse, France, June 2−6, 1996; pp 439−446.
(7) Javanmardi, J.; Nasrifar, K.; Najibi, S. H. Economic evaluation of natural gas hydrate as an alternative for natural gas transportation. *Appl. Therm. Eng.* **2005**, *25*, 1708–1723.
(8) Najibi, H.; Rezaei, R.; Javanmardi, J.; Nasrifar, K.; Moshfeghian, M. Economic evaluation of natural gas transportation from Iran's South-Pars gas field to market. *Appl. Therm. Eng.* **2009**, *29*, 2009–2015.
(9) Saito, Y.; Kawasaki, T.; Kondo, T.; Hiraoka, R. Methane storage in hydrate phase with water soluble guests. Proceeding of the 2nd International Conference on Gas Hydrate, Toulouse, France, June 2−6, 1996; pp 459−465.
(10) Zhong, Y.; Rogers, R. E. Surfactant effect on the hydrate formation. *Chem. Eng. Sci.* **2000**, *55*, 4175–4187.
(11) Kang, S. P.; Lee, H. Recovery of CO_2 from flue gas using gas hydrate: Thermodynamic verification through phase equilibrium measurements. *Environ. Sci. Technol.* **2000**, *34*, 4397–4400.
(12) Ganji, H.; Manteghian, M.; Zadeh, K. S.; Omidkhah, M. R.; Mofrad, H. R. Effect of different surfactants on methane hydrate formation rate, stability and storage capacity. *Fuel* **2007**, *86*, 434–441.
(13) Okutani, K.; Kuwabara, Y.; Mori, Y. H. Surfactant effects on hydrate formation in an unstirred gas/liquid system: An experimental study using methane and sodium alkyl sulfates. *Chem. Eng. Sci.* **2008**, *63*, 183–194.
(14) Wang, W. X.; Bray, C. L.; Adams, D. J.; Cooper, A. I. Methane storage in dry water gas hydrates. *J. Am. Chem. Soc.* **2008**, *130*, 11608–11609.
(15) Luo, Y. T.; Zhu, J. H.; Fan, S. S.; Chen, G. J. Study on the kinetics of hydrate formation in a bubble column. *Chem. Eng. Sci.* **2007**, *62*, 1000–1009.

spray towers, bubble towers, etc., which were used to study the hydrate formation kinetics by Luo et al., Englezos et al., Vysniauskas and Bishnoi, and Gnanendran and Amin, respectively.[15−18]

In recent years, many advances have been reported on reactors for enhancing the gas hydrate formation.[19] Tajima et al. made use of a new hydrate reactor with a Kenics-type static mixer to continuously form CO_2 hydrate.[20] Takahiro reported a new pipe hydrate reactor in Japan Patent 323751.[21] Szymcek et al. developed a pilot-scale continuous-jet hydrate reactor.[22] It was reported that a fluidized-bed reactor was used to research the formation and growth of CO_2 hydrate particles by Yamasaki et al.[23] Eaton et al. designed a novel high-pressure apparatus named FISH that was suitable for forming hydrates while allowing visual observations and accurate measurements of temperature and pressure conditions that accompany phase changes during the entire hydrate-forming process.[24] Moreover, some analyses for designing a new hydrate reactor were also reported. Mori and Komae evaluated the relation between the rate of guest-gas supply and the rate of actual guest-gas uptake into hydrates in a semi-batch- or batch-type reactor.[25] McCallum et al. studied the effect of the pressure vessel size on the formation of gas hydrates, and Tajima et al. minutely analyzed the mechanical mixing functions of static mixers for increasing the gas hydrate formation.[26,27] Several questions of hydrate reactor scale-up for industrialization were discussed with respect of the configurations of the reactor and the means of eliminating hydrate heat by Rogers et al.[28] In addition, Mori had proposed earlier a model parameter to evaluate the capability of different types of gas hydrate reactors in 2003.[29] Although there have been many advances on hydrate reactors, it is necessary to develop and research novel hydrate reactors.

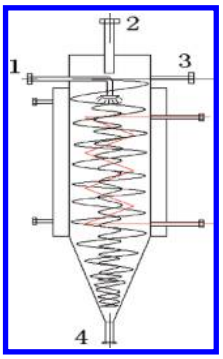

Figure 1. Flow filed and structure sketch of VIR: (1) ice slurry or water inlet, (2) unreacted gas outlet, (3) feed gas inlet, and (4) solid and liquid mixture outlet.

In this paper, a new CO_2 gas hydrate formation technology with a vortex and impinging stream reactor was reported, which was abbreviated as VIR. The vortex and impinging stream technology is one of high gravity or named Higee, which was originally proposed by Ramshow in the process of researching the microgravity field for National Aeronautics and Space Administration (NASA) in 1976.[30−33] In the reactor, violent vortex and impinging streams come into being and can enhance the mass transfer in reactants. As Figure 1 illustrates, the main structure of VIR is a cylinder, which can bear an inner pressure up to 25 MPa, and consists of a jacket cooler outside, a special figure multiple serpentine cooler inside, a sprayer for ice slurry or water at the top, and a conical head at the bottom. The empty volume of the reactor is 1.76 L, excluding the accessories. In the CO_2 hydrate formation process, the flow of gas is continuous and ice slurry or water is the disperse phase. Gas is introduced into VIR along the tangent of the inner circle at high speed through the gas inlet, and ice slurry or water is squirted from the sprayer at the top of the VIR. Then, two vortexes come into being near the inner wall and at the center. Before the unreacted gas is discharged from the gas outlet, it impinges against the ice slurry or water below the sprayer at the top of the VIR, which makes an impinging stream filed. Under the impact of the two vortexes and an impinging stream, the ice slurry or water stream will be turned into film, thread, and tiny drops by two kinds of mechanism forces named centrifugation and collision, which can intensify highly surface renewal and mixing in reactants. Especially, the centrifugal acceleration in the field near the reactor wall is hundreds of times the value of gravity acceleration, which generates a huge force field named Higee. A dimensionless parameter β, named the Higee factor, is defined as the ratio of the value of the centrifugal acceleration to that of

(16) Englezos, P.; Kalogerakis, N.; Dholabhai, P. D. Kinetics of gas hydrate formation from mixtures of methane and ethane. *Chem. Eng. Sci.* **1987**, *42*, 647–2666.
(17) Vysniauskas, A.; Bishnoi, P. R. A kinetics study of methane hydrate formation. *Chem. Eng. Sci.* **1983**, *38*, 1061–1072.
(18) Gnanendran, N; Amin, R. Modelling hydrate formation kinetics of a hydrate promoter−water−natural gas system in a semi-batch spray reactor. *Chem. Eng. Sci.* **2004**, *59*, 3849–3863.
(19) Bai, J.; Liang, D. Q.; Li, D. L.; Fan, S. S. Research progress on nature gas hydrate reactors. *Petrochem. Technol. China* **2008**, *137*, 1083–1088.
(20) Tajima, H.; Yamasaki, A.; Kiyono, F. Continuous formation of CO_2 hydrate via a Kenics-type static mixer. *Energy Fuels* **2004**, *18*, 1451–1456.
(21) Takahiro, K. Manufacturing method and apparatus of gas hydrate. Japan Patent 323751, 2001.
(22) Szymcek, P.; McCallum, S. D.; Taboada-Serrano, P.; Tsouris, C. A pilot-scale continuous-jet hydrate reactor. *Chem. Eng. J.* **2008**, *135*, 71–77.
(23) Yamasaki, A.; Takano, S.; Fuji, M.; Yanagisawa, Y.; Tajima, H.; Kiyono, F. Formation and growth of CO_2 hydrate particles in a fluidized bed reactor. *Abstr. Pap. Am. Chem. Soc.* **2003**, *225*, 852–853.
(24) Eaton, M.; Mahajan, D.; Flood, R. A novel high-pressure apparatus to study hydrate−sediment interactions. *J. Pet. Sci. Eng.* **2007**, *56*, 101–107.
(25) Mori, Y. H.; Komae, N. A note on the evaluation of the guest-gas uptake into a clathrate hydrate being formed in a semibatch- or batch-type reactor. *Energy Convers. Manage.* **2008**, *49*, 1056–1062.
(26) McCallum, S. D.; Riestenberg, D. E.; Zatsepina, O. Y.; Phelps, T. J. Effect of pressure vessel size on the formation of gas hydrates. *J. Pet. Sci. Eng.* **2007**, *56*, 54–64.
(27) Tajima, H.; Yamasaki, A.; Kiyono, F. Effects of mixing functions of static mixers on the formation of CO_2 hydrate from the two-phase flow of liquid CO_2 and water. *Energy Fuels* **2005**, *19*, 2364–2370.
(28) Rogers, R. E.; Zhong, Y.; Arunkumar, R.; Etheridge, J. A.; Pearson, E.; McCown, J.; Hogancamp, K. Gas hydrate storage progress for natural gas. Gas TIPS Winter, 2005; pp 14−18.
(29) Mori, Y. H. Recent advances in hydrate-based technologies for natural gas storage—A review. *Chem. Ind. Eng. Soc. China* **2003**, *54*, 1–17.
(30) Bucklin, R. W.; Won, K. W. Higee contactors for selective H_2S removal and superdehydration. Laurance Reid Gas Conditioning Conference, University of Oklahoma, Norman, OK, March 1987; pp 1−2.
(31) Ramshaw, C.; Mallinson, R. H. U.S. Patent 4,283,255, 1981.
(32) Sievers, M.; Gaddis, E. S.; Vogelpoh, A. Fluid dynamics in an impinging-stream−stream reactor. *Chem. Eng. Process.* **1995**, *34*, 115–119.
(33) Mohr, R. J. The role of Higee technology in gas processing. Gas Processing Association (GPA) Meeting, Dallas, TX, 1985.
(34) Budhijanto, B. Reaction engineering study of natural gas hydrate formation in special packed-bed reactors by controlling the boundary layer surfaces of the gas−liquid−solid phases. Ph.D. Dissertation, West Virginia University, Morgantown, WV, 2003.

gravity acceleration, which can represent the magnitude of the Higee field in VIR.[34]

$$\beta = \frac{2u^2}{D_i g} \quad (1)$$

$$u = \frac{V_{g,in}}{A_{g,in}} \quad (2)$$

$$A_{g,in} = \frac{\pi}{4} d_{g,in}^2 \quad (3)$$

where u is the velocity of the feed gas in VIR along the tangent of inner circle (m/s), D_i is the inner diameter in VIR (m), $V_{g,in}$ is the factual volume flow rate in the gas inlet under the specified experimental conditions (m^3/s), $A_{g,in}$ and $d_{g,in}$ are the acreage and diameter of the nozzle of CO_2 gas inlet (m^2 and m), respectively.

Besides the structure of VIR, the contribution of the mechanism forces also depends upon the properties of the target fluids, such as viscosity, velocity, and mutual miscibility. Once applied to hydrate formation, the mechanisms could enhance the mixing of the water and guest gases and, consequently, could realize an effective hydrate formation process. The advantages of using VIR for the hydrate formation process are as follows:[35−37] (a) The structure of VIR is simple and close to axial symmetry without intricate accessories, which would be easy in the scale-up to an industrial production. (b) Without mobile parts in VIR, the seal of the equipment in the hydrate formation process becomes very easy under the conditions of high pressure and low temperature. Therefore, a safer process can be achieved, which can avoid explosion of flammable gases and is crucial for hydrate formation using natural gas. (c) The VIR is compact in structure, which would occupy little space. Because of the characters in the geometry structure, the VIR would be suitable for a continuous process of gas hydrate formation. (d) The VIR can be operated by means of a multiple-stage series, which would increase the gas hydrate formation rate and gas capacity.

Despite the above advantages, no study on the hydrate formation process has been conducted with VIR, and consequently, no information is available in the literature on the hydrate formation process using VIR. Therefore, the formation processes of a hydrate in VIR were investigated experimentally with a laboratory-scale experimental apparatus in this paper, focusing on the effect of a dimensionless parameter β, which is related to the flow velocities of the feed gas on the hydrate formation patterns. CO_2 was used as the guest molecule for hydrates, considering the application of the present hydrate formation process to an ocean disposal scenario in the form of CO_2 hydrates.

2. Experimental Section

2.1. Experimental Equipment. Figure 2 shows a process flow diagram of the experimental apparatus for the hydrate formation, which can consist of six parts as follows: (a) The CO_2 gas circulation system consists of the high-pressure CO_2 gas bottle, gas storage and buffer vessel, gas compressor, and correlative pipes and valves, which are made of stainless steel. In addition, the maximum working pressure of the system is 10 MPa. (b) The transportation system for ice slurry consists of the pump used to transport ice slurry, an ice slurry tank with a cooler inside, and some related pipes and valves, which are made of stainless steel. The maximum working pressure of the system is 10 MPa. The pump belongs to a high-pressure diaphragm type, and the maximum flow flux and the maximum output pressure are 400 L/h and 20 MPa, respectively. (c) The VIR detailed description has been given in the Introduction. Its inner diameter is 100 mm. (d) The cooling system includes the VIR jacket cooler, inner serpentine coolers, ice slurry tank serpentine coolers, CO_2 gas cooler, and correlative pipes and valves. The refrigerant is alcohol solution in this system, and the lowest temperature can reach 255 K. (e) The heart equipment in the separator system for the solid−liquid mixture is the separator with a special accessory inside used to separate the mixture of hydrate solid and unreacted ice slurry. (f) The computer and data acquisition system includes three types of transducers, such as temperature, pressure, and volumetric flow rate, a set of data acquisition instruments, and a computer that can record all of the real-time data during the experiment. The accuracies of the temperature sensors, pressure transducers, and volumetric flow transducers are ±0.2 K, ±10 KPa, and ±0.15 L/h, respectively.

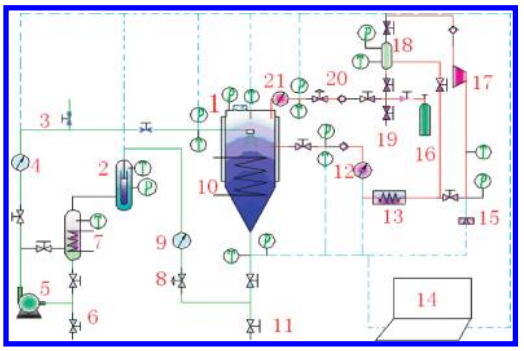

Figure 2. Process flow diagram of hydrate formation with VIR: (1) VIR, (2) solid−liquid separator, (3) ice slurry sampling valve, (4) inlet ice slurry flow meter, (5) ice slurry pump, (6) draining valve, (7) ice slurry tank, (8) regulating valve, (9) outlet solid−liquid mixture flow meter, (10) inner cooler, (11) draining valve, (12) inlet gas flow meter, (13) gas cooler, (14) computer and data acquisition system, (15) safety valve, (16) high-pressure CO_2 gas bottle, (17) gas compressor, (18) gas storage and buffer vessel, (19) vent valve, (20) pressure regulating valve, and (21) outlet gas flow meter.

Table 1. Experimental Materials Used in This Work

material	purity	supplier
CO_2 gas	≥99.999 wt %	Hua Te Gas Co., Ltd., China
pure water		distilled

2.2. Experimental Material. In this work, pure water was made through a double-distilled process. Then, it was frozen into an ice block in a low-temperature chamber, which was grinded into ice powder using a small attrition mill. Finally, the ice powder was collected by the method of sieving, whose average diameter of particle size was less than 0.833 mm. The experimental materials were listed in Table 1.

2.3. Experimental Procedure. First, each equipmental unit was washed with distilled water, evacuated, and purged with CO_2 gas sequentially to make sure that the system was thoroughly clean and air was absent. After the cooling system began to run, ice powder already made was put into the ice slurry tank. Then, the valves in the CO_2 gas circulation system were turned

(35) Munjal, S.; Dudukovic, M. P.; Ramachandran, P. Mass-transfer in rotating packed beds—I. Development of gas−liquid and liquid−solid mass-transfer correlations. *Chem. Eng. Sci.* **1989**, *44*, 2245–2256.

(36) Munjal, S.; Dudukovic, M. P.; Ramachandran, P. Mass-transfer in rotating packed beds—II. Experimental results and comparison with theory and gravity flow. *Chem. Eng. Sci.* **1989**, *44*, 2257–2268.

(37) Lekse, J.; Taylor, C. E.; Ladner, E. P. The impinging-stream reactor: A high performance loop reactor for mass transfer controlled chemical reactions. *Chem. Eng. Sci.* **1992**, *47*, 2877–2882.

Table 2. Values of β, u, P_r, T_r, γ_{CO_2}, n_{in}, n_{out}, w_{in}, and w_{out} in This Work

run	Higeer factor β	u (m/s)	P_r (MPa)	T_r (K)	γ_{CO_2} (mol/h)	n_{in} (mol/h)	n_{out} (mol/h)	w_{in} (h^{-1})	w_{out} (h^{-1})
1	14.98	2.77	2.357	274.7	12.4	173.4	161.0	150	148.5
2	20.16	3.21	1.790	274.9	20.5	145.6	125.1	150	147.6
3	30.65	3.95	3.163	274.8	31.6	348.3	316.7	150	146.4
4	42.29	4.64	2.415	274.9	44.3	276.8	232.5	150	145.0
5	53.83	5.24	1.938	274.8	66.3	286.3	220.0	150	142.8
6	77.88	6.30	2.956	275.5	85.4	538.3	452.9	150	140.1
7	126.40	8.03	2.357	275.4	121.8	506.6	384.8	300	287.2
8	187.16	9.77	2.365	275.6	155.6	615.6	460.0	300	283.5
9	217.53	10.54	2.953	275.5	178.6	924.9	746.3	300	281.2
10	244.59	11.17	2.300	275.3	194.6	732.3	537.7	300	279.6
11	300.70	12.29	2.805	275.4	213.5	945.9	732.4	300	277.5
12	352.00	13.40	2.910	275.5	235.2	997.6	762.4	300	275.4
13	390.28	14.11	3.140	275.9	249.8	1149.7	899.9	300	273.8

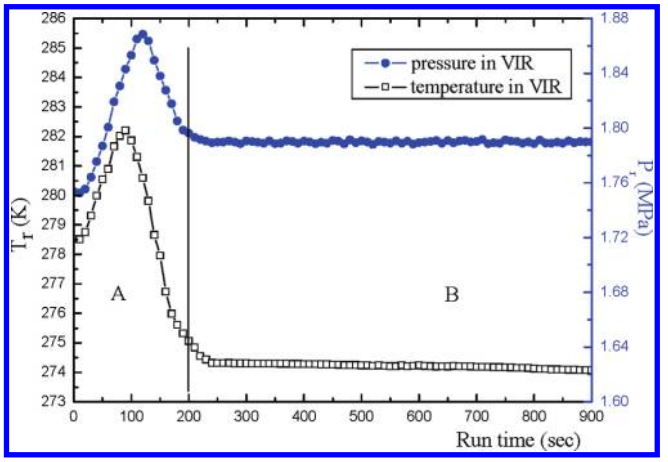

Figure 3. Change process of T_r and P_r at $\beta = 20.16$.

on, and CO_2 gas was introduced until the system pressure reached a desired experimental value. When the temperature in the VIR reached a desired value, the acquisition system started to record the data. Then, the gas compressor was started. In succession, the diaphragm pump was started and the ice slurry was introduced into the system. Finally, the CO_2 hydrate began to form and flowed out from the outlet at the bottom of the VIR with the unreacted ice slurry. Most of the CO_2 hydrates were held in the separator, and the unreacted ice slurry flowed into the ice slurry tank. The unreacted CO_2 gas flowed out from the outlet at the top of the VIR, entering into the gas storage and buffer vessel and taking part in the hydrate reaction with the fresh CO_2 gas from the high-pressure gas bottle again. Once the temperature in the VIR increased from the stable value, the pump and gas compressor ceased and this experiment was finished at the same time.

The CO_2 hydrate formation is an exothermic reaction, and the melting of ice is an endothermic process; therefore, the existence of ice powder was used to eliminate rapidly the heat of the hydrate reaction in this work.[38] The mass fraction of ice in the ice slurry in the VIR inlet was about 13.539 wt % by means of the calorimetric measurement.[39] The two ice slurry flow rates were regulated in the experiments. One was 300 L/h when the Higee factor β was more than 100, and another was 150 L/h when the Higee factor β was less than 100. The inlet CO_2 gas flow rate could be changed by adjusting the system pressure and the motor rotational frequency of the gas compressor. Moreover, the valves in the system stayed open to ensure that the system continuously ran during the experiment. To keep the pressure in the VIR, the valves in the gas outlet pipe from the VIR are opened less than those in the gas inlet.

The CO_2 gas consumption rate γ_{CO_2} under the specified experimental conditions was calculated as follows:[15,34]

$$\gamma_{CO_2} = n_{g,in} - n_{g,out} \tag{4}$$

$$n_{g,in} = 3600\frac{P_{g,in}V_{g,in}}{Z_{in}RT_{g,in}} \tag{5}$$

$$n_{g,out} = 3600\frac{P_{g,out}V_{g,out}}{Z_{out}RT_{g,out}} \tag{6}$$

The gas flow rate can be calculated with eqs 7 and 8 between the real application condition and the calibration condition, which were supplied by manufacturers.

$$V_{g,in} = V_{o,g,in}\sqrt{\frac{\rho_o P_{g,in} T_o}{\rho_{g,in} P_o T_{g,in}}} \tag{7}$$

$$V_{g,out} = V_{o,g,out}\sqrt{\frac{\rho_o P_{g,out} T_o}{\rho_{g,out} P_o T_{g,out}}} \tag{8}$$

where $n_{g,in}$ and $n_{g,out}$ are the molar number flow rates of CO_2 in the gas inlet and outlet (mol/h), respectively, $V_{o,g,in}$, $V_{o,g,out}$, $V_{g,in}$, and $V_{g,out}$ are the values of the volume flow rate of the instrument and the fact in the gas inlet and outlet (m^3/s), respectively, ρ_o is the density of N_2 gas under the conditions of P_o (6 MPa) and T_o (283 K), in which the gas flow meters are calibrated (kg/m^3), $\rho_{g,in}$, $\rho_{g,out}$, $P_{g,in}$, $P_{g,out}$, $T_{g,in}$, and $T_{g,out}$ are the density of CO_2 gas, pressure, and temperature in the gas inlet and outlet (kg/m^3, MPa, and K), respectively, Z_{in} and Z_{out} are the compressibility factors in the gas inlet and outlet, which can be calculated using the Benedict−Webb−Rubin equation, respectively, and R is the universal gas constant.

3. Results and Discussion

3.1. Formation Process of CO_2 Gas Hydrate in the VIR. As shown in Table 2 and Figures 3−8, the formation process of CO_2 gas hydrate in the VIR has been investigated under the conditions of the pressures ranging from 1.79 to 3.163 MPa and the temperature ranging from 274.7 to 275.9 K, in which the P_r, T_r, w_{in}, and w_{out} are the pressure and temperature in the VIR and the volume flow rate of the ice slurry inlet and outlet, respectively.

All of the process curves in Figures 3−8 have a ridge at the beginning period and gradually become a horizontal line later. At the beginning of the formation process, there are four reasons that result in the temperature increase in the

(38) Moudrakovski, I. L.; Ratcliffe, C. I.; McLaurin, G. E. Hydrate layers on ice particles and superheated ice: A ^{1}H NMR microimaging study. *J. Phys. Chem. A* **1999**, *103*, 4969–4972.

(39) Qing, C. Y.; Song, W. J.; Xu, J. Q.; Xiao, R.; Dong, K. J.; Feng, Z. P. Study on the solid fraction measurement of TBAB clathrate hyrate slurry (CHS) using a conductance probe. *Chin. J. Sci. Instrum.* **2009**, *30*, 542–547.

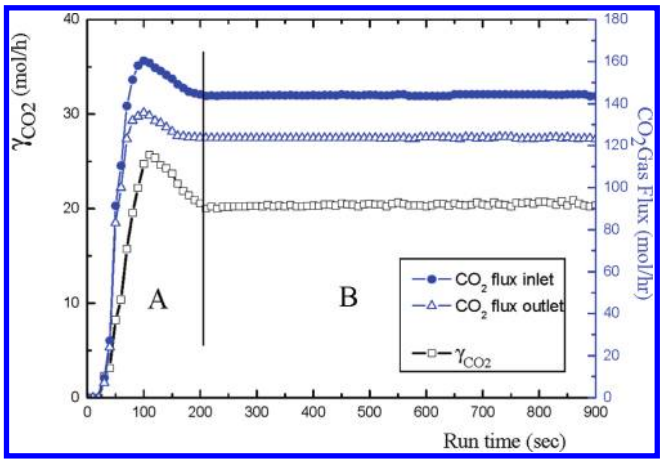

Figure 4. Change process of $n_{g,in}$, $n_{g,out}$, and γ_{CO_2} at $\beta = 20.16$.

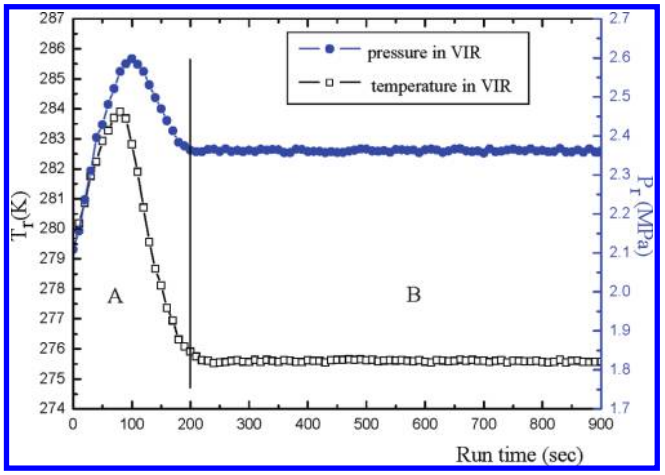

Figure 5. Change process of T_r and P_r at $\beta = 187.16$.

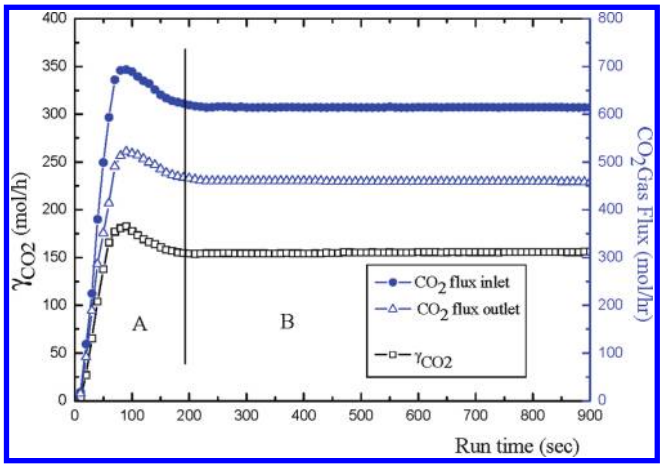

Figure 6. Change process of $n_{g,in}$, $n_{g,out}$, and γ_{CO_2} at $\beta = 187.16$.

reactor. The first factor is that the unit apparatus outside the VIR does not have enough capacity to cool the CO_2 gas that flows fast to the desired temperature. The second results from the effect of the gas compressor, which can release compression heat and inhale much fresh CO_2 gas without being refrigerated completely. The third is the slightly lag start of the ice slurry system, which causes the heat not to be removed in time. The fourth comes from the hydrate reaction heat. When the temperature rises to a certain value, it will

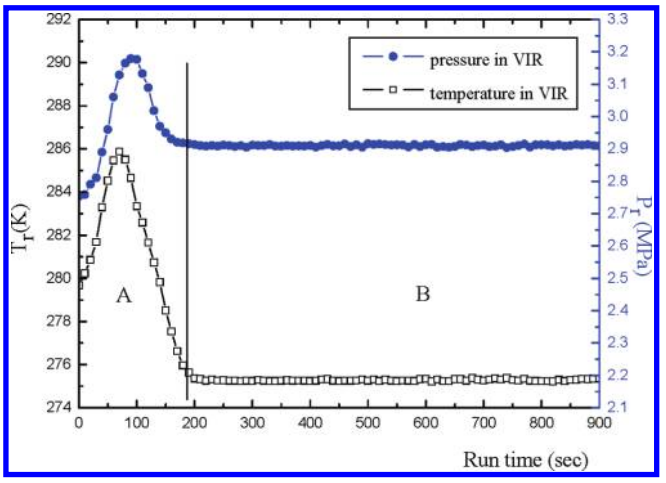

Figure 7. Change process of T_r and P_r at $\beta = 352.0$.

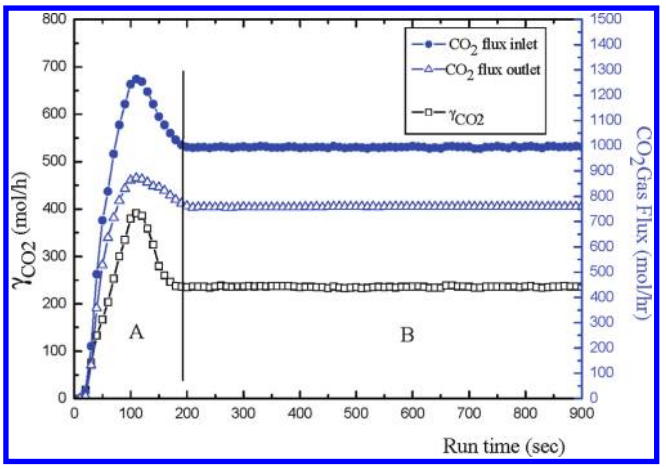

Figure 8. Change process of $n_{g,in}$, $n_{g,out}$, and γ_{CO_2} at $\beta = 352.0$.

lead to more ice particles to melt and absorb a greater quantity of heat. About 200 s later, the temperature in the VIR is stable, which is attributed to a balance between the endothermic process of ice thaw and the exothermic process of the hydrate reaction, compression heat, and fresh CO_2 gas cooling. Although the change process of the pressure in the VIR was similar to that of the temperature, there is some difference between them. In the beginning, the gas quantity that is supplied by the gas compressor is more than the consumption, which causes the CO_2 gas to accumulate and the pressure to increase in the VIR. The peak of the pressure curve appeared slightly later than that of the temperature curve, perhaps because of the gas expansion and contraction in the temperature change process. The CO_2 gas molar flux curves are also similar to those of the temperature and pressure change processes. CO_2 gas is consumed gradually with the CO_2 hydrate formed, which makes the CO_2 gas molar flux decrease. In the B zone, the gas consumption reaches equilibrium with that supplied in the VIR and the CO_2 hydrates are formed stably and rapidly. The difference of the CO_2 gas molar numbers charged into and discharged out of the VIR represented the CO_2 consumption rate γ_{CO_2}, which is an important parameter in experiments.

From Figures 3 to 8, the values of β are 20.16, 187.16, and 352.0, respectively. It can be found that the peak values of T_r and P_r became larger by degrees in the A zone with the increase of the Higee factors β. The reason is speculated that

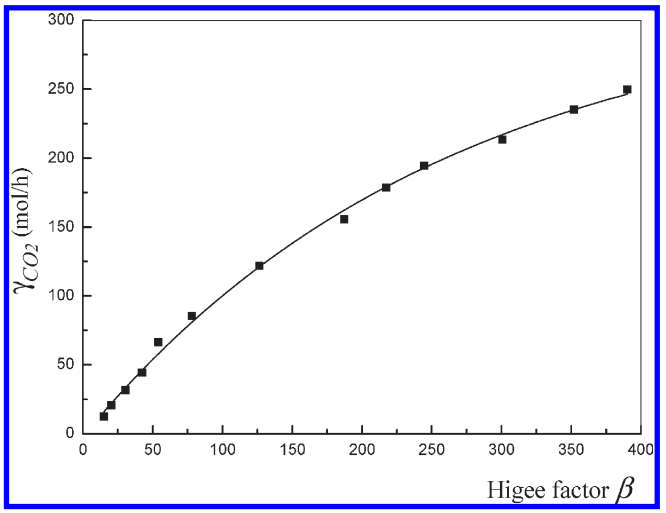

Figure 9. Dependence of the gas hydrate formation rate γ_{CO_2} on the Higee factor β.

the more fresh CO_2 gas was brought into the VIR by the gas compressor with the increase of the Higee factors β. The same was the CO_2 gas consumption rate γ_{CO_2}, which was also listed in Table 2.

Through the analysis above, it is concluded that the formation process of CO_2 gas hydrate in the VIR has two steps. One is the unstable hydrate formation process, which is in the A zone and occupies about 200 s. In this period, the initial point of CO_2 hydrate formation is not confirmed because of the limit of the experimental apparatus. The other is a stable one, which is in the B zone and the main one to be noticed. There are two balances in the period, such as heat equilibrium between the endothermic process of ice thaw and the exothermic process of the hydrate reaction, compression heat and fresh CO_2 gas cooled, and mass equilibrium between the supply and the consumption of CO_2 gas. Especially, the CO_2 gas hydrate can be formed rapidly and continuously in the period. As shown in Figures 3−8 and Table 2, the CO_2 gas consumption rate γ_{CO_2} becomes larger with the increase of the Higee factors β in the B zone. The conclusion can be deduced that the Higee factors β can affect the CO_2 gas hydrate formation in the system.

3.2. Influence of the Higee Factor β on the CO_2 Gas Hydrate Formation Rate γ_{CO_2}. Figure 9 shows that the CO_2 gas hydrate formation rate γ_{CO_2} increases with the increase of Higee factor β. When the value of β is less than 50, the value of γ_{CO_2} is no more than 50 mol/h. In contrast, when the Higee factor β is more than 80, γ_{CO_2} increases approximately linearly. The uptrend of γ_{CO_2} decreases gradually in Figure 9, which indicates that there is a possible limit of γ_{CO_2} with the Higee factor β increase. According to the fluid-flow study on the rotating packed bed from Guo et al. and Burns and Ramshaw, when the value of the Higee factor β was less than 60 in the flow field, the fluid flowed in the pattern of film. However, when the Higee factor β value was more than 100, the disperse phase existed in the pattern of tiny drops and thread.[40,41] Therefore, the centrifugal and impinging forces can be small in the Higee factor β less than 50, but they are enough to break and disperse the ice slurry when the Higee factor β was more than 100. In other words, it can also illustrate that the Higee field supplied by VIR is able to intensify the mass transfer.

In the experiment, the maximum value of the CO_2 gas hydrate formation rate γ_{CO_2} was up to 249.8 mol/h when the Higee factor β was 390.28. It was shown that the Higee factor β could affect the CO_2 gas hydrate formation rate and the mechanism functions supplied by the VIR could promote the CO_2 gas hydrate formation under the experimental conditions. According to the paper reported by Taboada-Serrano et al., the experimental uncertainties were analyzed.[42] In the experiment, the error margins of the CO_2 gas hydrate formation rate γ_{CO_2} were about 0.7% and came from the accuracies of the temperature sensors, pressure transducers, and volumetric flow transducers, which were 0.1, 0.1, and 0.15%, respectively.

4. Conclusion

In this work, a VIR system was proposed to enhance the CO_2 gas hydrate formation, where a high-gravity field could be generated. In the VIR, there are two violent vortex and impinging streams and their resulting huge forces can intensify the mass transfer in reactants. Through the study on the formation process of CO_2 gas hydrate in the VIR, it can be shown that there are two steps in the process. One is the unstable hydrate formation process. The other is stable, and the CO_2 gas hydrate was formed rapidly and continuously in the process. In the VIR, the mechanism functions of centrifugal and impinging forces can affect the CO_2 gas hydrate formation. The CO_2 hydrate formation rate γ_{CO_2} increases with an increasing Higee factor β, which represents the magnitude of the high-gravity field. When the Higee factor β is 390.28, the maximum formation rate of the CO_2 gas hydrate is up to 249.8 mol/h.

Acknowledgment. The authors are grateful to the National Natural Science Foundation of China (50706056), National Basic Research Program of China (2009CB219504), Chinese Academy of Science (CAS) (KGCX2-YW-805), and Guangdong Science and Technology Project of China (2009B030600005).

(40) Guo, F.; Zheng, C.; Guo, K.; Feng, Y. D.; Gardner, N. C. Hydrodynamics and mass transfer in cross-flow rotating packed bed. *Chem. Eng. Sci.* **1997**, *52*, 3853–3859.

(41) Burns, J. R.; Ramshaw, C. Process intensification: Visual study of liquid maldistribution in rotating packed beds. *Chem. Eng. Sci.* **1996**, *51*, 1347–1352.

(42) Taboada-Serrano, P.; Ulrich, S.; Szymcek, P.; McCallum, S. D.; Phelps, T. J.; Palumbo, A.; Tsouris, C. Multiphase, microdispersion reactor for the continuous production of methane gas hydrate. *Ind. Eng. Chem. Res.* **2009**, *48*, 6448–6452.